

# High Resolution Structure of the Large Ribosomal Subunit from a Mesophilic Eubacterium

Joerg Harms<sup>1,5</sup> Frank Schluenzen,<sup>1,5</sup>  
Raz Zarivach,<sup>2,5</sup> Anat Bashan,<sup>2</sup> Sharon Gat,<sup>2</sup>  
Ilana Agmon,<sup>2</sup> Heike Bartels,<sup>1</sup> François Franceschi,<sup>3</sup>  
and Ada Yonath<sup>1,2,4</sup>

<sup>1</sup>Max-Planck-Research Unit for Ribosomal  
Structure

Notkestrasse 85  
22603 Hamburg  
Germany

<sup>2</sup>Department of Structural Biology  
Weizmann Institute  
76100 Rehovot  
Israel

<sup>3</sup>Max-Planck-Institute for Molecular Genetics  
Ihnestrasse 73  
14195 Berlin  
Germany

## Summary

We describe the high resolution structure of the large ribosomal subunit from *Deinococcus radiodurans* (D50S), a gram-positive mesophile suitable for binding of antibiotics and functionally relevant ligands. The overall structure of D50S is similar to that from the archae bacterium *Haloarcula marismortui* (H50S); however, a detailed comparison revealed significant differences, for example, in the orientation of nucleotides in peptidyl transferase center and in the structures of many ribosomal proteins. Analysis of ribosomal features involved in dynamic aspects of protein biosynthesis that are partially or fully disordered in H50S revealed the conformations of intersubunit bridges in unbound subunits, suggesting how they may change upon subunit association and how movements of the L1-stalk may facilitate the exit of tRNA.

## Introduction

Ribosomes are the universal ribonucleoprotein complexes that translate the genetic code into proteins. They are built of two independent subunits that associate upon the initiation of protein biosynthesis. The large ribosomal subunit (1.45 MDa) is responsible for the formation of the peptide bond, provides the sheltered path for the nascent proteins, and participates in the translocation event. It consists of two RNA chains (called 23S and 5S) and over 30 proteins. The natural tendency of ribosomes to deteriorate, their conformational heterogeneity, and their internal flexibility pose difficulties in their crystallization. The key for obtaining crystals suitable for crystallographic studies was the use of robust ribosomes, assuming that they deteriorate less while being prepared and therefore expected to yield more homogeneous starting materials for crystallization. Indeed, the

only high resolution structures determined so far are of the small subunit from *Thermus thermophilus*, T30S (Schluenzen et al., 2000; Wimberly et al., 2000) and the large one from *Haloarcula marismortui*, H50S (Ban et al., 2000).

Crystals of complexes of H50S with substrate or transition stage analogs led to a suggestion for a putative catalytic mechanism exclusively exploiting the ribosomal RNA (Nissen et al., 2000). This mechanism was soon challenged biochemically (Barta et al., 2001; Bayfield et al., 2001), and it was shown that all the nucleotides said to be crucial for the catalytic activity according to it, could be mutated with little or no effect on peptide bond formation in vitro (Polacek et al., 2001) and in vivo (Thompson et al., 2001). In addition, several features known to be involved in the various noncatalytic functions of the large subunit were found to be disordered in the 2.4 Å structure of H50S (Ban et al., 2000; Yusupov et al., 2001).

We therefore initiated crystallographic studies of the large ribosomal subunit from *Deinococcus radiodurans*, an extremely robust gram-positive eubacterium, the ribosome of which shows striking sequence similarity to *T. thermophilus* and *E. coli* (White et al., 1999). *D. radiodurans* was originally identified as a contaminant of irradiated canned meat. Later, it was isolated from environments that are either very rich or extremely poor in organic nutrients, such as soil and animal feces, weathered granite in a dry Antarctic valley, room dust, wastes from atomic piles, and irradiated medical instruments. It is the most radiation-resistant organism currently known. It survives under conditions that cause DNA damage, such as hydrogen peroxide, and ionizing or ultraviolet radiation. It contains systems for DNA repair, DNA damage export, desiccation, starvation recovery, and genetic redundancy (White et al., 1999).

*D. radiodurans* is sensitive to all clinically important antibiotic agents targeting the ribosome (Schluenzen et al., 2001), contrary to halophilic ribosomes (Mankin and Garrett, 1991). Since most of the antibiotic agents interact with the peptidyl transferase center or hamper the path of the nascent protein chains, investigating their binding modes to D50S should assist the elucidation of the ribosomal catalytic mechanism (Schluenzen et al., 2001). Here, we describe the structure of D50S at 3.1 Å resolution, obtained from crystals of the 50S subunit from *D. radiodurans* (D50S) that were grown and kept under conditions that are almost identical to those maintaining optimal biological activity. We focus on novel structural elements seen in this structure as well as on features that have conformations that differ from their counterparts in H50S (Ban et al., 2000) or in the large subunit within the T70S ribosome (Yusupov et al., 2001).

## Results and Discussion

We determined and refined the 3.1 Å structure of the 50S subunit (Table 1 and Figure 1) from *Deinococcus radiodurans*, by a combination of molecular replacement

<sup>4</sup> Correspondence: ada.yonath@weizmann.ac.il

<sup>5</sup> These authors contributed equally to this work

Table 1. Structure Determination

Set	Resolution (Å)	R <sub>sym</sub> (%)	Observed/Unique ref	Completeness (%)	<I/sig (I)>	
Native	50–3.0	14.5 (44.0)	4,787,954 / 441,570	95.0 (48.5)	7.3 (1.8)	
Native-a*	50–2.9	12.2 (45.6)	5,510,777 / 340,493	59.9 (28.3)	6.5 (1.5)	
Heavy-atom	# of sites	Resolution (Å)	Unit Cell (Å)	R <sub>sym</sub> (%)	Completeness (%)	<I/sig (I)>
Penta-Ir	56	50–4.0	170.24 410.54 696.52	14.5 (47.2)	93.9 (90.9)	5.8 (1.9)
W12	48 = 4 × 12	30–6.0	170.15 408.65 696.52	8.1 (12.9)	71.9 (69.2)	14.1 (5.0)

\*Included in the table to indicate potential crystal quality. Space group = I222; Unit Cell = 170.8, 409.4, 695.6 Å. R/R<sub>free</sub> = 24.0%/27.4%. Values for the highest resolution bins (3.05–3.0 Å or 2.95–2.9 Å) are given in parentheses. FOM = 0.58 (0.54) at 50–4.0 Å (4.37–4.0 Å) after phasing with SHARP, and 0.78 after density modification with SOLOMON.

and MIRAS phasing. Ninety-six percent of the nucleotides and most of the amino acid residues of the 33 proteins of D50S (Figure 2) were traced in the electron density map. Among the 33 proteins, three are less well resolved, but significant portions of them could be traced. We also detected the sites of several hydrated Mg<sup>2+</sup> ions. The detailed analysis of the structure will be published elsewhere.

#### Overall Structure of D50S

The traditional shape of the large ribosomal subunit, as seen by electron microscopy (Penczek et al., 1999; Mueller et al., 2000), contains a massive large core with a central elongated feature and two lateral protuberances, called the L1 and L7/L12 stalks. The view, frequently referred to as the “crown view,” looks like a halved pear with two protuberances. Its flat surface (“front side”) faces the small subunit in the 70S ribosome and its round back side faces the solvent. The overall shape of the large ribosomal subunit from *D. radiodurans* (Figure 1) is similar to the traditional view as well as to the structures of H50S (Ban et al., 2000) and that of the 50S part of the 70S ribosome (Yusupov et al., 2001). The

lateral protuberances, however, seem to be flexible, and several orientations have been detected for them (see below).

The 23S RNA forms the bulk of the structure and the small 5S RNA forms most of an elongated feature in the center of the crown. On the secondary structure level, the two RNA chains form seven domains (Figure 1). Each of these domains has a defined three-dimensional shape and together they produce a fairly compact intertwined structure, in contrast to the domain-like design of the 30S subunit (Schluenzen et al., 2000; Wimberly et al., 2000).

The gross similarity of the rRNA folds of D50S to the available 50S structures allowed its superposition onto that of the 23S RNA in the 2.4 Å structure of H50S (Ban et al., 2000) and of the 50S subunit within the 5.5 Å structure of the T70S ribosome (Yusupov et al., 2001). Although the RNA fold and the overall protein distribution are rather similar in the three structures, we detected significant structural differences even within the conserved regions, which cannot be explained solely by expected phylogenetic variations. In order to pinpoint the meaningful differences, we divided the model into

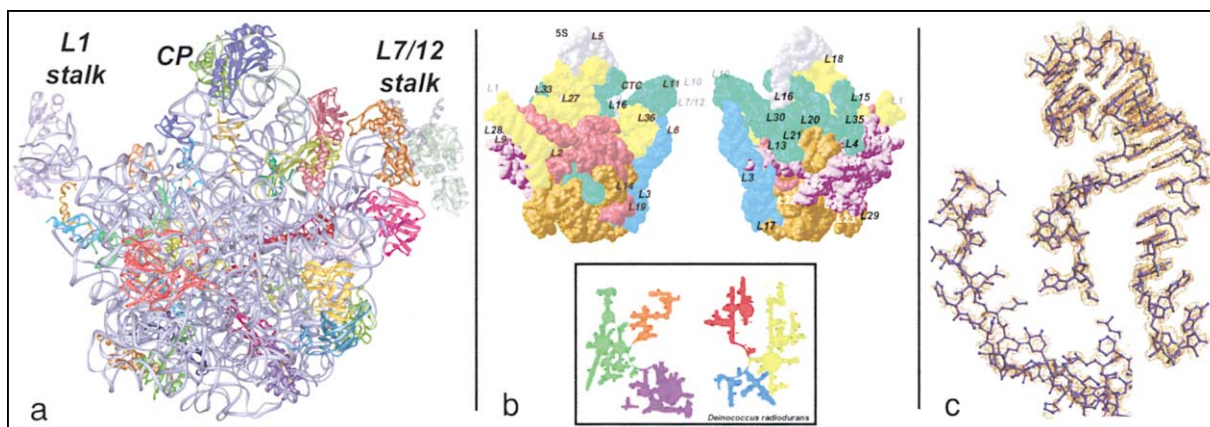


Figure 1. The D50S Model and the Electron Density Maps

(a) The crown view representation of D50S structure, shown from the side facing the small subunit within the 70S ribosome. The RNA chains are shown as silver ribbons and the protein main chains in different colors. The L7/L12 stalk is on the right, the L1 stalk is on the left, and the central protuberance (CP), including the 5S RNA is in the middle of the upper part of the particle. The semitransparent proteins are less well resolved.

(b) Top: the RNA domain organization of D50S together with the approximate positions of all D50S proteins, designated by their numbers. Left: same view as in (a); right: the solvent side. The domain-coloring scheme is according to the diagram of the proposed RNA secondary structure (bottom).

(c) Typical segments of the electron density Fourier map. Top: H1 (domain I); bottom: protein L31. Both features are absent in the H50S model. Contour levels: 1.7  $\sigma$  for the RNA and 1.2 for the protein.

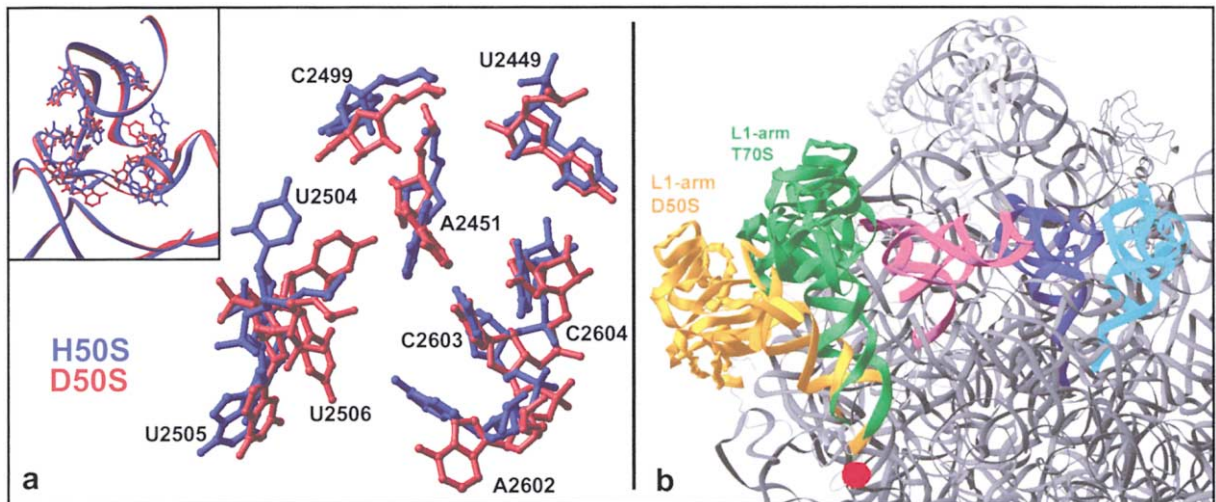


Figure 2. The PTR and a Possible Movement of the L1 Stalk

(a) Nucleotides within the PTR that show different orientations in D50S and H50S. Insert: the overall fold of the PTR, shown in a slightly different orientation in order to emphasize the back-bone similarity.  
 (b) Part of the D50S structure (as gray ribbons). The L1-arm of D50S is highlighted (in gold). Also shown is the L1-stalk of T70S (green) and protein L1 of T70S (dark green) and the potential location of protein L1 in D50S (yellow-gold). In T70S, the L1-arm and protein L1 block the exit of the E-tRNA (magenta), whereas in D50S, the L1-arm swings around a pivot point (marked by a red dot) by  $\sim 30^\circ$ .

individual structural elements, each containing a few neighboring helices and junctions, checked the environment of each element separately, and compared it with its counterparts in H50S and T70S (Supplemental Table S1, available online at <http://www.cell.com/cgi/content/full/107/5/679/DC1>).

Almost all D50S proteins are built from globular domains and extended loops or tails. Only a few are built exclusively of globular domains or extended features. As in the 30S subunit (Schluenzen et al., 2000; Wimberly et al., 2000) and in H50S (Ban et al., 2000), most of the globular domains of the D50S proteins are peripheral, located on the solvent side of the subunit, and their extensions permeate the interior of the particle. The flat front side that interfaces the small subunit within the assembled ribosome is almost free of globular domain of proteins. A few proteins however, do not have extensions and are built of more than a single globular domain. These have special positions in the D50S subunit. They are located either at the ends of functionally important protuberances (L1, L7/L12, L10, and L11) or fill a gap between the central protuberance and one of the stalks (CTC).

In contrast to the significant similarity between the RNA fold of D50S and H50S, the protein folds show remarkable differences, even when sharing homology with their counterparts in H50S (Supplemental Table S1). In addition, D50S contains several proteins that have no counterparts in H50S. Of structural interest is a three domains protein (CTC), an extended  $\alpha$ -helical protein (L20), and two Zn-finger proteins (L32 and L36). Analysis of the general modes of the RNA-protein interactions within D50S did not reveal striking differences from what was reported for the other ribosomal particles. However, most of the D50S proteins that have counterparts in H50S show significantly different conformations.

#### The Peptidyl Transferase Center and Its Vicinity

The peptidyl transferase activity of the ribosome has been linked to a multibranch loop in the 23S secondary structure diagram of domain V, known as the peptidyl transferase ring (PTR). From the 43 nucleotides forming the PTR in *D. radiodurans*, 36 are conserved in *H. marismortui*. Superposition of the backbone of the high resolution structures of the PTR nucleotides in the two species (Ban et al. 2000, and PDB 1JJ2) shows a similar fold (rmsd of 1.02 Å). The orientations of some of the nucleotides, however, show distinct differences (Figure 2). These include a translational shift of the sugar moieties that maintain coplanar bases but are pointing in different directions in the two structures, as well as different degrees of rotation with hardly any change in the sugar moieties. Among the PTR conserved nucleotides, A2062, C2063, C2064, U2449, A2451, C2499, U2504, G2505, and U2506 (*E. coli* numbering) display rotational or translational shifts of above 2 Å. The largest rotational differences are between the base moieties of A2451 (86 degrees), A2506 (79 degrees), and U2504 (40 degrees).

A2451 is the key element in the peptide bond catalysis mechanism, which was proposed based on the structure of H50S (Ban et al., 2000, Nissen et al., 2000). Biochemical evidence has shown the functional importance of U2504 and U2506. U2504 has been implicated in the binding of the 3' end of the aminoacyl tRNA prior to peptide bond formation (Porse and Garrett, 1995; Hall et al., 1988) and U2506 was shown to be protected from chemical modification by P site tRNA (Moazed and Noller 1987). It is possible, however, that the different orientations or locations of these bases reflect the flexibility needed for the formation of the peptide bond. It is also conceivable that the different orientations of these bases result from the differences in the functional states of H50S and D50S, since it has been shown that struc-

tural changes occur at distinct nucleotides of the peptidyl transferase ring upon transition between the active and inactive conformations (Bayfield et al., 2001).

In unbound D50S, as in H50S, the peptidyl transferase center seems to be clear of proteins. L27 is one of the only proteins located in the interface area of D50S. Its globular domain was detected at the base of the central protuberance, consistent with many of the results of immunoelectron microscopy, cross-linking, affinity labeling, chemical probing, mutations, and footprinting (Sonenberg et al., 1973; Wower et al., 1998; A. Mankin, personal communication). This protein has been shown to influence the peptidyl transferase activity in *E. coli* 50S by a variety of experimental observations, including antibiotic cross-linking (Bischof et al., 1995) and a deletion mutant that shows deficiencies in the peptidyl transferase activity and impaired enzymatic binding of Phe-tRNA Phe to the A site (Wower et al., 1998). It has been proposed that protein L27 plays a role in mediating the proper placement of the 3' end of the A site tRNA at the peptidyl transferase center, screening the negative charge of the tRNA molecules from that of the ribosomal RNA during the peptidyl transferase reaction, and influencing the interactions of the 3' end of deacylated tRNA with the ribosome after peptidyl transfer.

Based on the positions of the docked tRNA molecules according to the 5.5 Å structure of the T70S/tRNA complex (Yusupov et al., 2001), protein L27 can interact with the P site tRNA. H50S does not have protein L27 or any homologous counterpart, and the protein that occupies the place of L27 is L21e. Contrary to L27, the tail of L21e folds backward, toward the interior of the subunit, disabling potential contacts with the P site tRNA. In D50S, the N-terminal tail of L27 is disordered. However, it might play a more direct role in the positioning of the CCA end of the A and/or P site tRNA. It remains to be seen if within the assembled ribosome, the N-terminal tail of L27 reaches the vicinity of the peptidyl transferase center.

### The L1 Stalk

The L1 stalk includes helices H75–H78 and protein L1, which can function as a transcriptional repressor in the cytoplasm by binding to its own mRNA (Nikonov et al., 1996). The absence of the L1 protein has a negative effect on the rate of protein synthesis (Subramanian and Dabbs, 1980). In the complex of T70S with three tRNA molecules, the L1 stalk interacts with the elbow of E-tRNA. This interaction, together with protein S7 of the small subunit, blocks the exit path for the E-tRNA (Yusupov et al., 2001). Consequently, it was suggested that the release of the deacylated tRNA requires that one or both of these features move (Yusupov et al., 2001). In H50S, the entire L1 arm is disordered and therefore could not be traced in the electron density map (Ban et al., 2000)—an additional hint of the inherent flexibility of this feature.

In D50S, the RNA helices of the L1 stalk have a similar fold to that seen in T70S. However, the entire L1 stalk in the unbound D50S is tilted by about 30 degrees away from its position in the T70S ribosome, so that the distance between the outermost surface points of the L1 arm in the two positions is over 30 Å (Figure 2). The

location of protein L1 in D50S does not block the presumed exit path of the E site tRNA. It is possible that the mobility of the L1 arm is utilized for facilitating the release of E site tRNA. Although the orientation of the L1 arm in the 70S ribosome during the release of the E site tRNA is still not known, the two defined orientations that have been observed indicated that movement of the L1 arm might occur during protein biosynthesis. Superposition of the structure of D50S on that of the T70S ribosome allowed the definition of a pivot point for the possible movement of the L1 arm. Differences found in the relative orientation of the L1 stalk have been correlated with the presence or absence of tRNA and elongation factors (Gomez-Lorenzo et al., 2000). Although there is no evidence showing that the L1 stalk in the 70S ribosome assumes the conformation seen in the unbound D50S, it is conceivable that the two positions represent part or all of the conformational change required for the release of the E site tRNA. Movement may also provide an alternative explanation for the previous cryo-EM location of the E site (Agrawal et al., 2000), and explain the appearance of an extra density in the vicinity of the L1 arm at the 7.5 Å cryo-EM map of the 50S subunit (Mueller et al., 2000).

### The L7/L12 Stalk and the GTPase Center

A major protruding region of domain II that extends from the solvent to the front surface of the large subunit consists of H42–H44 and proteins L7/L12 and L10. This stalk has been shown to be involved in the contacts with translational factors, and in factor-dependent GTPase activity (Chandra Sanyal and Liljas, 2000). In D50S, the location of this stalk is somewhat shifted (by 3–4 Å) compared to its position within the 70S ribosome (Yusupov et al., 2001). In the 2.4 Å structure of H50S (Ban et al., 2000), the entire L7/12 stalk is disordered. However, a recently deposited entry to the Protein Data Bank (PDB 1JJ2) includes coordinates of H42–H44, the RNA portion of the stalk, which shows a rotation of about 12 degrees from its position in D50S. Observing this stalk in three different locations is consistent with the flexibility associated with its involvement in EF-G-dependent translocation (Agrawal et al., 2001). Assignment of each of the positions to a specific functional state still awaits the elucidation of high resolution structures of 70S ribosomes at the relevant states.

L11, a highly conserved ribosomal protein, which is associated with the GTPase-associated region, is located at the base of the L7/L12 stalk. L11 and the antibiotic thiostrepton bind cooperatively to a highly conserved segment of 23S RNA (Cundliffe et al., 1979; Ryan et al., 1991) that has been probed by several biophysical, crystallographic, NMR, and electron-microscopy techniques (Hinck et al., 1997; Conn et al., 1999; Wimberly et al., 1999; GuhaThakurta and Draper, 2000; Agrawal et al., 2001). The crystal structure of a complex containing L11 together with a 58 nucleotide RNA chain mimicking the RNA stretch that binds it within the *E. coli* 50S subunit (Wimberly et al., 1999), showed tight binding of the C-terminal domain of L11, but limited contacts between its N-terminal domain and the RNA. Therefore, it was proposed to function as a conformational switch. In D50S, the separation between the two domains of

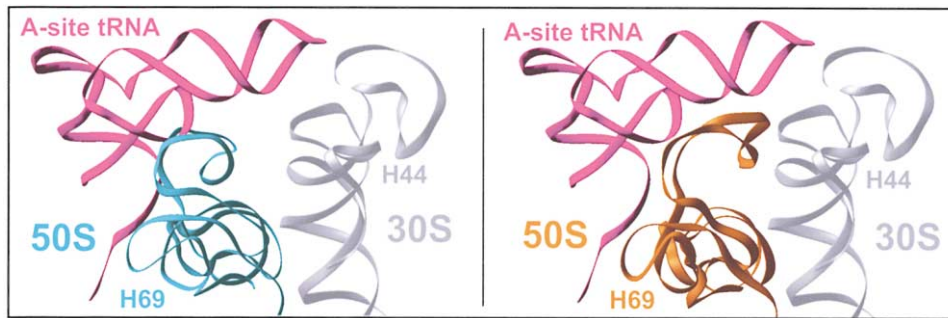


Figure 3. The Intersubunit Bridge to the Decoding Region

Left: H69 in the unbound D50S subunit (in cyan) and the corresponding feature in the 70S ribosome (gold). The figure indicates the proposed movement of H69 toward the decoding center of H44 (gray) in T30S, as a consequence of a collision with the A site tRNA.

protein L11 is somewhat larger than that observed in the isolated structures, as well as in the assembled T70S (Yusupov et al., 2001), thus supporting the dynamic aspect of this proposal.

#### Intersubunit Bridges

The constituents of the intersubunit bridges between the large and small subunits within the ribosome were seen in the T70S structure (Yusupov et al., 2001). Many of them are resolved in the map of D50S, but found to be disordered in H50S (Yusupov et al., 2001; Ban et al., 2000). Since the structure of H50S was determined earlier, the disorder of its features led to the notion that all structural elements involved in intersubunit bridges or in other functionally relevant contacts are disordered in unbound large subunits. These become stabilized in the 70S ribosome by their interactions with the small subunit and with the tRNA molecules (Yusupov et al., 2001). The finding that the same functional features are of defined conformations in the unbound D50S indicates that the crystal structure of H50S contains features that are more flexible than that of D50S, possibly because the crystallized H50S subunits underwent environmentally induced conformational changes. These could result from the exchange of the 3 M KCl, the main component of the *H. marismortui* in situ environment (Ginzburg et al., 1970), by reduced amounts (1.5 M) of NaCl (Ban et al., 1999, 2000).

An example is the only intersubunit bridge (B1b) that is constructed solely from proteins (Yusupov et al., 2001), S13, which is located in the head of the small subunit, and a domain of L5, which is missing in H50S, but fully resolved in D50S. An additional striking example, is the universally conserved stem-loop of H69 (domain IV), which is the main component of the bridge between the large subunit and the decoding area in the small one (bridge B2a). The orientation of H69 in D50S, that represents the unbound large subunit, differs from that seen within the entire ribosome, T70S, so that the distance between the tips of the stem-loops of H69 in T70S and in D50S is about 13.5 Å. H69 is located on the surface of the intersubunit interface. In the 70S ribosome, it stretches toward the small subunit, whereas in the free 50S, it makes more contacts with the large subunit (H71). Comparison of the two orientations of H69 (Figure 3) led us to propose that a modest swing of H69 in the

free 50S subunit is sufficient for moving this helix into a bridging position, so that it can stretch out and interact with the small subunit near the decoding center. In this position, H69 can also contact the A and P site tRNA molecules, and be proximal to elongation factor EF-G in the posttranslocation state (Yusupov et al., 2001). This swing and the consequent stretching out may be triggered by the contacts of H69 with the initiator P site tRNA, which being a part of the initiation complex, is carried into its position simultaneously with subunit association, and occupies part of the space that in the unbound subunit is occupied by H69. A feature that is not fully resolved in both D50S and H50S structures is H38 (domain II), called the “B1a bridge” or “A finger,” of which 15 and 27 bases are disordered, respectively.

Proteins L14 and L19 form an extended interprotein  $\beta$  sheet, composed of two  $\beta$ -hairpin loops of L14 and L19 (Figure 4a). In H50S, L24e, though smaller in size, is located at the same position as L19 in D50S and forms a similar  $\beta$  sheet element. Both L14 and L19 are directly involved in the formation of intersubunit bridges. L19 is known to make contacts with the penultimate stem of the small subunit, at bridge B6, and L14 forms bridge B8. It is therefore possible that the structural element produced by L14 and its counterpart (L19 or L24e) has functional relevance in the construction of these two bridges. In D50S, these proteins together with protein L3 form one of the two intimately connected protein clusters, consistent with a large number of reported cross-links (Walleczek et al., 1989). This clustering may enhance the stability of the structural features required for the intersubunit bridges.

#### The Nascent-Protein Exit Tunnel

More than three decades ago, biochemical studies showed that the newest synthesized part of a nascent protein is masked by the ribosome (Malkin and Rich, 1967; Sabatini and Blobel, 1970). In the mid eighties, a feature that may account for these observations was first seen as a narrow elongated region in images reconstructed at very low resolution (60 Å) in 80S ribosomes from chick embryos (Milligan and Unwin, 1986) and at 45 Å in images of 50S subunits of *Bacillus stearothermophilus* (Yonath et al., 1987). Despite the low resolution, these studies showed that this tunnel spans the large subunit from the location assumed to be the pepti-

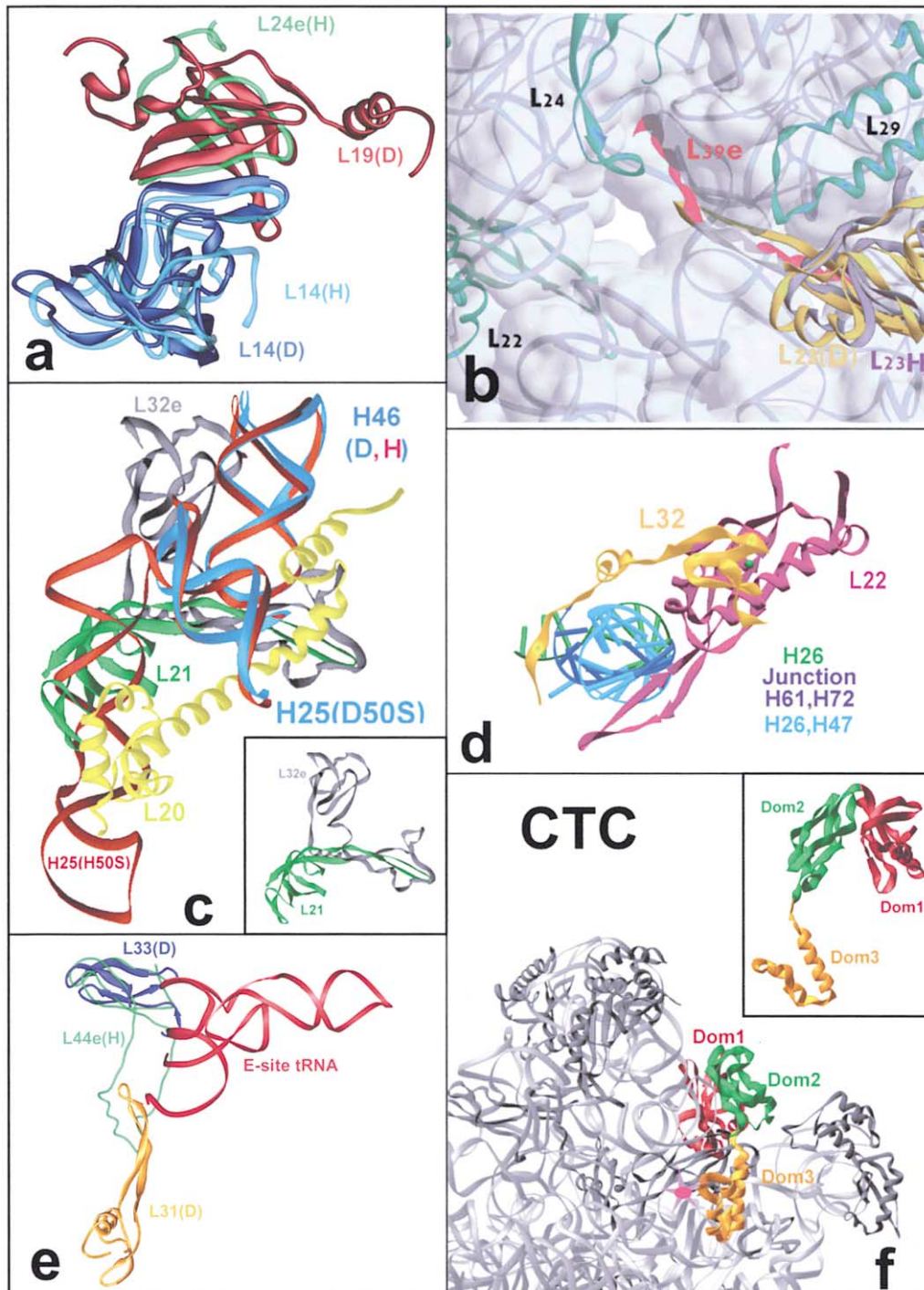


Figure 4. Novel Structural Features in D50S

(a) The interprotein  $\beta$  sheet, made by proteins L14–L19 in D50S (involved in intersubunit bridges B8 and B6, respectively), overlaid on the H50S counterparts, L14 and HL24e. Note the differences in structure and size between L19 in D50S to HL24e.

(b) The opening of the nascent polypeptide tunnel. The D50S protein L23, its substitutes in H50S, L39e, and HL23, are highlighted.

(c) Overlay of H25 in D50S on H50S. In D50S, H25 is significantly shorter, and proteins L20 and DL21 are attached to it. Their space is occupied by part of the long helix H25 in H50S. Insert: only proteins L21 and L23e, that are related by an approximate 2-fold, are shown.

(d) A tweezers-like structure is formed by proteins L32 and L22, presumably stabilizing a helical construct, generated from three RNA domains: H26, the junction H61, 72 and the junction H26, H47.

(e) Overlay of the D50S protein L33 and L44e shows similar globular domain folds, but no extension exists for L33. Part of the space of the HL44e loop is occupied by the extension of DL31. E site tRNA is interacting with DL33 and HL44e and L31 loop.

(f) The crown view front side is shown (RNA as gray ribbons). The N-terminal domain of CTC (Dom1) is located at the solvent side, behind the CP. The middle domain (domain 2) wraps around the CP, and fills the gap to the L11 arm. The C-terminal domain (domain 3) is located at the rim of the intersubunit interface and reaches the site of docked A site tRNA position (marked by a red-dotted pink star). Insert: a side view of CTC (obtained by a rotation of about  $90^\circ$  around the long axis of the view shown in Figure 1).

dyl transferase site to its lower part, and that it is about 100 Å in length and up to 25 Å in diameter (Yonath et al., 1987), as confirmed later at high resolution in H50S (Nissen et al., 2000) and in D50S.

The structural features building the walls of the tunnel, their chemical composition, and the “nonstick” character in H50S are described in (Nissen et al., 2000). We found the same characteristics in D50S—lack of well-defined structural motifs, large patches of hydrophobic surfaces, and low polarity. The opening of this tunnel at its exit site is located at the bottom of the particle. In H50S, it includes two proteins, L31e and L39e, that do not exist in D50S. L39e is a small protein of an extended nonglobular conformation that replaces the tail of L23 in D50S and penetrates deeper than the tail of L23 in D50S, into the RNA features that construct the walls of the tunnel in that region (Figure 4b).

L39e is present in archaea and many eukaryotes, but not in eubacteria. It seems that with the increase in cellular complexity, a better control on the tunnel’s opening is required, and for this two proteins (L23 and L39e) replace a single one (L23 of D50S). A protein in this delicate position may provide the communication path between the ribosome and other cell components. Providing this feature is conserved, in eukaryotes it may act as a hook for the ribosome on the ER membrane. A high resolution structure of a eukaryotic ribosome, bound to the ER membrane, should provide an answer to these open questions.

#### Specific Features and Replacements between Species

Helix H25 (of domain II) is the 23S rRNA helix showing the greatest length variability among the 3 phylogenetic domains (Gutell, 1996). Its length varies from 4 to 891 nucleotides. It contains 27 nucleotides in D50S and 74 in H50S. The common 27 nucleotides have the same orientation and location in the two structures. However, the region that is occupied by this helix in H50S and not in D50S, hosts, in the latter, two proteins, L20 and L21 (Figure 4c). These two proteins exist in all known eubacterial ribosomes, but not in H50S. L21 has a small β-barrel-like domain that is connected to an extended loop. L20, in contrast, is built of a long, α-helical extension. Its shape and location make L20 a perfect candidate for RNA organization. This may explain why L20 is one of the early assembly proteins, and why it can take over the role of L24 in mutants lacking the latter. This exchange between proteins and RNA seems not to reduce the stabilization of this region, since protein L32e has a looped tail, sufficient in length to compensate for many of the contacts made by the tail of L20 and the loop of L21 (Figure 4c). It is therefore possible that the loop of L32e organizes the RNA environment in H50S in a fashion similar to the loop of L21 in D50S. The globular domains of protein L32e and L21 appear to be similar, and it is possible that L21 and L32e are indeed related. The globular domain of L32e is rotated by 180 degrees around an axis defined through its tail, and the space that in D50S is occupied by L21, is occupied in H50S by the extension of H25.

#### Protein Tweezers

Among the proteins that appear in D50S and have no replacements or counterparts in H50S are two Zn-finger

proteins, L32 and L36. The position occupied by L32 in D50S overlaps that hosting the loop of L22 in H50S, and in *D. radiodurans*, L32 and L22 form a tweezers-like motif that seems to clamp the interactions between the junctions of H26/H47 of domains II and III respectively, and H61/H72 of domain IV (Figure 4d). These two proteins interact extensively with protein L17 that occupies the location of L31e in H50S, and the entire region seems to be highly stabilized. The question, still to be answered is: why was a protein replaced by a loop of another one (or vice-versa), when this replacement seems to cause changes in a well-organized structural motif.

#### Extended Loops that Bind the E Site tRNA

The E site tRNA interacts in D50S, with the end of the extended loop of protein L31. In H50S, the region interacting with E site tRNA is provided by the extended loop of L44e. These two proteins are located at the two opposite sides of the docked E site tRNA, yet the interactions occur in approximately the same place, utilizing their extended loops (Figure 4e). In D50S, L33 that has no extended loop occupies the space taken by the globular domain of L44e in H50S, and the globular domains of both are rather similar. These complicated rearrangements may indicate that the ribosomes developed different pathways in order to preserve the configurations and locations of the functionally relevant features.

#### A Three-Domain Version of L25

In D50S, the protein replacing L25 in *E. coli* and its homolog in TL5 in T50S is called CTC. H50S contains neither L25 nor any of its homologs. Of the known members of the TL5 family, that from *D. radiodurans* is the longest. It contains 253 residues, about 130 more than L25 (*E. coli*) and 40 more than TL5 (*T. thermophilus*). The D50S CTC has three domains. Whereas the folds of the N-terminal and the middle domains of CTC can be related to those of L25 (Lu and Steitz, 2000) and TL5 (Fedorov et al., 2001), which have been determined at isolation, the structure of its C-terminal domain is novel and was determined from the D50S map. We also found that the relative orientations of the N-terminal and the middle domains of CTC differ from that determined for the two domains of TL5 in complex with a 40-nucleotide fragment of the 5S RNA.

The N-terminal domain of CTC is located on the solvent side of D50S (Figure 4f). The middle domain fills the space between the 5S RNA and the L11 arm and interacts with H38, the helix forming the intersubunit bridge called B1a. The interactions of the middle domain of CTC with H38, and the partial wrapping of the central protuberance (CP) may provide additional stability. The C-terminal domain of CTC is placed at the rim of the intersubunit interface, so that its C terminus reaches the A site. The somewhat lower quality of the electron density map of this domain may indicate its inherent flexibility, and hint at its possible involvement in the regulation of the binding and the release of A site tRNA.

#### Concluding Remarks

The availability of two high-resolution structures of unbound large ribosomal subunits from species of different

phylogenetic kingdoms, the archaeal H50S and eubacterial D50S, opened the way for comparative studies.

The large subunit has a compact structure. Its core is built of well-packed interwoven RNA features and it is known to have less conformational variability than the small subunit. Nevertheless, it does possess various conformations that can be correlated to the functional activity of the ribosome. Based on the comparison between the structures of the free D50S and of the bound T50S, we propose that the ribosome utilizes the inherent flexibility of its features for facilitating specific tasks. Remarkable examples are helix H69, which creates the 50S hook to the decoding region of the small subunit, and the entire L1 arm, that produces the revolving gate for the exiting tRNA molecules.

The striking difference between the conservation of the RNA folds and the significant diversity of the ribosomal proteins indicates that the latter are not just gluing together RNA features and maintaining the intricate RNA fold. Their additional tasks include binding of factors and substrates and the enhancement of intersubunit association. The extended protein termini and the long protein loops are mainly buried within the particle and thus are trapped in distinct conformations. However, those that are pointing toward the solution, such as protein S18 in the small subunit (Pioletti et al., 2001) or the loop of L5, maintain a high level of flexibility and are available to interact, to bind, and to enhance the placement of factors and substrates. It is therefore conceivable that in such cases, the diversity of ribosomal proteins is linked to the structural variability of the interacting components. On the other hand, remarkable preservation of structural motifs was observed in some ribosomal proteins despite their overall conformational and sequence differences. The example of L14/L19 interprotein  $\beta$  sheet (Figure 4a) and its H50S counterpart L14/L24e shows how similar functional requirements are satisfied in different ribosomes.

#### Experimental Procedures

Cells were grown as recommended by the ATCC in the ATCC medium 679, with minor modifications. Ribosomes and their subunits were prepared as described in Noll et al., 1973.

Crystals were obtained by vapor diffusion at 18°C, by equilibrating solutions containing the same buffer used for testing their in vitro functional activity (10 mM MgCl<sub>2</sub>, 60 mM NH<sub>4</sub>Cl, 5 mM KCl, 10 mM HEPES [pH 7.8]), and minute amounts (0.1%–1%) of poly- and monovalent alcohols (typically equal to 0.2:0.7% dimethylhexandiol:ethanol) against the same solutions but with twice the amount of the alcohols. For optimizing crystal growth, the exact conditions had to be determined for every preparation individually. The same or similar divalent alcohols (e.g., ethyleneglycol) were used as cryo protectants for flash freezing of the crystals in liquid propane.

X-Ray diffraction data were collected at 95K with well-collimated X-ray beams, at SR stations that provide high brightness (ID14/ESRF/EMBO and ID19/APS). We screened the crystals at BW6/MPG and BW7/EMBL at DESY. The data were recorded on image-plates (MAR 345) or CCD (Mar, Quantum 4, or APS2) and processed with DENZO and reduced with SCALEPACK (Otwinowski and Minor, 1997) and the CCP4 package (Bailey, 1994).

Heavy-atom derivatives were prepared by soaking 1–2 mM of iridium pentamide or K<sub>5</sub>H(PW<sub>12</sub>O<sub>40</sub>)<sub>12</sub>H<sub>2</sub>O, for 24 hr. Experimental MIRAS phases were obtained from anomalous data. The tungsten and iridium sites were obtained from difference Patterson, residual, and difference Fourier maps.

#### Phase Determination

Preliminary phases were assigned by molecular replacement, with AmoRe (Navaza, 1994), using the 50S structure from *Haloarcula marismortui* as a basis for the search model. The ribosomal proteins of H50S have a very low sequence homology to their counterparts in D50S. Therefore, they were removed from the search model. A large part of the sequence and the secondary structure of the RNA chains are rather similar in both species, hence, only regions with a particularly low homology (e.g., bases 670–700, H25 and H38) were removed as well. The resulting search model, comprising about 60% of the structure of a 50S subunit, was sufficient to obtain a unique solution in the rotation and translation searches, resulting in a correlation of 45.8% and an R factor of 49.8%.

The calculation of a  $2F_o - F_c$  Fourier map based on these initial phases did not yield an interpretable electron density. After density modification with SOLOMON (Abrahams and Leslie, 1996), the electron density was sufficient to trace a significant part of the structure. The resulting model phases were used to readily locate the heavy atom sites of two heavy atom derivatives (Table 1). The addition of MIRAS phase information obtained from the two derivatives using SHARP (de La Fortelle and Bricogne, 1997) dramatically improved the quality of the electron density map (Figure 1), so that we could unambiguously trace essentially all the RNA (96%) and all ribosomal proteins except for parts of L1, L10, and L7/L12. These three proteins could still be located in the electron density map, though they are less well resolved. The structure was further refined in CNS, yielding an  $R_{\text{factor}}/R_{\text{free}}$  of 24.0%/27.4%.

#### Structure Determination

The genome of *D. radiodurans* has been determined (White et al., 1999), but no ribosomal proteins have been sequenced at the amino-acid level. We therefore separated the ribosomal proteins and identified them on 2D gels and by sequencing the five N-terminal amino acids of each protein. Some discrepancies were found when compared with the DNA sequences (TIGR database; White et al., 1999), among them protein CTC starts at residue 19, and protein L6 that starts at residue 30 of the predicted sequence.

As no secondary structure was predicted for the ribosomal RNA, we constructed a secondary structure diagram for the 23S and 5S RNA chains of D50S (Figure 1), guided by their sequences and the available diagram for the RNA of the 50S subunit from *Thermus thermophilus* (Gutell, 1996) and the RNA cross-links database (Baranov et al., 1999). We traced the 23S and 5S rRNA chains manually in the electron density map, using the program O (Jones et al., 1991), and on comparing their fold to the predicted diagram, we found remarkable agreement. Only in a few places did the base-pairing system deviate from the predicted scheme. An example is the predicted base pair near the loop of H81 of domain V (C2243–G2255, in *D. radiodurans* numbering system) that was found to be flipped out in the three-dimensional structure of D50S.

The few D50S proteins that share homology with their counterparts in H50S were identified in our map. However, all had to be retraced. The placement of proteins L17, CTC (replacing L25 in *E. coli*), L27, L28, L31, L32, L33, L34, L35, and L36 that do not exist in H50S, was benefited from the great similarity between *D. radiodurans* and *E. coli* and utilized the vast amount of knowledge concerning the protein's relative positions (Wittmann, 1983; Walleczek et al., 1989) and their interactions with the rRNA (Ostergaard et al., 1998). We also made use of the coordinates determined by X-ray crystallography or NMR (Golden et al., 1993; Wimberly et al., 1999; GuhaThakurta and Draper, 2000; Fedorov et al., 1999, 2001; Worbs et al., 2000; Unge et al., 1998; Nikonov et al., 1996; Hoffman et al., 1996; Davies et al., 1996; Wahl et al., 2000; Hard et al., 2000; Nakashima, et al., 2001).

#### Docking Procedure

We placed the A, P, and E site tRNA molecules on the large ribosomal subunit, in the same relative orientation that was observed at 5.5 Å resolution of T70S (Yusupov et al., 2001), as described in Schluenzen et al., 2000.

#### Acknowledgments

We thank J.M. Lehn for indispensable advice; M. Pope for the tungsten clusters; M. Wilchek, W. Traub, A. Mankin, and A. Tocilij for

critical discussions; R. Wimmer for indicating the ribosome source; R. Albrecht, T. Auerbach, W.S. Bennett, Z. Biron, H. Burmeister, C. Brune, C. Glotz, M. Gluehmann, G. Goeltz, H.A.S. Hansen, M. Kessler, M. Laschever, S. Meier, J. Muessig, M. Peretz, M. Pioletti, C. Radzwill, B. Schmidt, and A. Wieweger for contributing to different stages of the research. These studies could not be performed without the cooperation of the staff of the synchrotron radiation facilities at EMBL and MPG at DESY; ID14/2 and 4 at EMBL/ESRF, and ID19/APS/ANL. Support was provided by the Max-Planck Society, the U.S. National Institutes of Health (GM34360), the German Ministry for Science and Technology (grant 05-641EA), and the Kimmelman Center for Macromolecular Assembly at the Weizmann Institute. A.Y. holds the Martin S. Kimmel Professorial Chair.

Received August 2, 2001; revised October 22, 2001.

## References

- Abrahams, J.P., and Leslie, A.G.W. (1996). Methods used in the structure determination of bovine mitochondrial F-1 ATPase. *Acta Crystallogr. D* 52, 30–42.
- Agrawal, R.K., Spahn, C.M.T., Penczek, P., Grassucci, R.A., Nierhaus, K.H., and Frank, J. (2000). Visualization of tRNA movements on the *E. coli* 70S ribosome during the elongation cycle. *J. Cell Biol.* 150, 447–459.
- Agrawal, R.K., Linde, J., Sengupta, J., Nierhaus, K.H., and Frank, J. (2001). Localization of L11 protein on the ribosome and elucidation of its involvement in EF-G-dependent translocation. *J. Mol. Biol.* 311, 777–787.
- Bailey, S. (1994). The CCP4 suite—programs for protein crystallography. *Acta Crystallogr. D* 50, 760–763.
- Ban, N., Nissen, P., Hansen, J., Capel, M., Moore, P.B., and Steitz, T.A. (1999). Placement of protein and RNA structures into a 5 Å resolution map of the 50S ribosomal subunit. *Nature* 400, 841–847.
- Ban, N., Nissen, P., Hansen, J., Moore, P.B., and Steitz, T.A. (2000). The complete atomic structure of the large ribosomal subunit at 2.4 Å resolution. *Science* 289, 905–920.
- Baranov, P.V., Kubarenko, A.V., Gurvich, O., Shamolina, T.A., and Brimacombe, R. (1999). The database of ribosomal crosslinks: an update. *Nucleic Acids Res.* 27, 184–185.
- Barta, A., Dorner, S., Polacek, N., Berg, M., and Lorsch, J.R. (2001). Mechanism of ribosomal peptide bond formation. *Science* 291, 203.
- Bayfield, M.A., Dahlberg, A.E., Schulmeister, U., Dorner, S., and Barta, A. (2001). A conformational change in the ribosomal peptidyl transferase center upon active/inactive transition. *Proc. Natl. Acad. Sci. USA* 98, 10096–10101.
- Bischof, O., Urlaub, H., Kruff, V., and Wittmann-Liebold, B. (1995). Peptide environment of the peptidyl transferase center from *E. coli* 70S ribosomes as determined by termoaffinity labeling with dihydrospiramycin. *J. Biol. Chem.* 270, 23060–23064.
- Chandra Sanyal, S., and Liljas, A. (2000). The end of the beginning: structural studies of ribosomal proteins. *Curr. Opin. Struct. Biol.* 10, 633–636.
- Conn, G.L., Draper, D.E., Lattman, E.E., and Gittis, A.G. (1999). Crystal structure of a conserved ribosomal protein-RNA complex. *Science* 284, 1171–1174.
- Cundliffe, E., Dixon, P., Stark, M., Stoffler, G., Ehrlich, R., Stoffler-Meilicke, M., and Cannon, M. (1979). Ribosomes in thiostrepton-resistant mutants of *B. megaterium* lacking a single 50 S subunit protein. *J. Mol. Biol.* 132, 235–252.
- Davies, C., White, S.W., and Ramakrishnan, V. (1996). The crystal structure of ribosomal protein L14 reveals an important organizational component of the translational apparatus. *Structure* 4, 55–66.
- de La Fortelle, E., and Bricogne, G. (1997). Maximum-likelihood heavy-atom parameter refinement for MIR and MAD methods. In *Methods in Enzymology*, R.M. Sweet and C.W. Carter, eds. (New York: Academic Press).
- Fedorov, R., Nevskaya, N., Khairullina, A., Tishchenko, S., Mikhailov, A., Garber, M., and Nikonov, S. (1999). Structure of ribosomal protein L30 from *Thermus thermophilus* at 1.9 Å resolution: conformational flexibility of the molecule. *Acta Crystallogr. D* 55, 1827–1833.
- Fedorov, R., Meshcheryakov, V., Gongadze, G., Fomenkova, N., Nevskaya, N., Selmer, M., Laurberg, M., Kristensen, O., Al-Karadaghi, S., Liljas, A., et al. (2001). Structure of ribosomal protein TL5 complexed with RNA provides new insights into the CTC family of stress proteins. *Acta Crystallogr. D* 57, 968–976.
- Ginzburg, M., Sacks, L., and Ginzburg, B.Z. (1970). Ion metabolism in *Halobacterium*. *J. Gen. Physiol.* 55, 178–207.
- Golden, B.L., Ramakrishnan, V., and White, S.W. (1993). Ribosomal protein L6: structural evidence of gene duplication from a primitive RNA binding protein. *EMBO J.* 12, 4901–4908.
- Gomez-Lorenzo, M.G., Spahn, C.M.T., Agrawal, R.K., Grassucci, R.A., Penczek, P., Chakraborty, K., Ballesta, J.P.G., Lavandera, J., Garcia-Bustos, J.F., and Frank, J. (2000). Three-dimensional cryo-electron microscopy localization of EF2 in the *Saccharomyces cerevisiae* 80S ribosome at 17.5 Å resolution. *EMBO J.* 19, 2710–2718.
- GuhaThakurta, D., and Draper, D.E. (2000). Contributions of basic residues to ribosomal protein L11 recognition of RNA. *J. Mol. Biol.* 295, 569–580.
- Gutell, R. (1996). Comparative sequence analysis and the structure of 16S and 23S rRNA. In: *Ribosomal RNA: Structure, Evolution, Processing and Function in Protein Biosynthesis* (A. Dahlberg, ed.) CRC Press, pp. 111–128.
- Hall, C., Johnson, D., and Coppermann, B.S. (1988). <sup>3</sup>H-p-azidopurpuro-mycin photo affinity labeling of *E. coli* ribosomes: evidence for site specific interaction at U2504 and G2502 in domain V of 23S RNA. *Biochemistry* 27, 3983–3990.
- Hard, T., Rak, A., Allard, P., Kloo, L., and Garber, M. (2000). The solution structure of ribosomal protein L36 from *Thermus thermophilus* reveals a zinc-ribbon-like fold. *J. Mol. Biol.* 296, 169–180.
- Hinck, A.P., Markus, M.A., Huang, S., Grzesiek, S., Kustovich, I., Draper, D.E., and Torchia, D.A. (1997). The RNA binding domain of ribosomal protein L11: three-dimensional structure of the RNA-bound form of the protein and its interaction with 23 S rRNA. *J. Mol. Biol.* 234, 1013–1020.
- Hoffman, D.W., Cameron, C.S., Davies, C., White, S.W., and Ramakrishnan, V. (1996). Ribosomal protein L9: a structure determination by the combined use of X-ray crystallography and NMR spectroscopy. *J. Mol. Biol.* 264, 1058–1071.
- Jones, T.A., Zou, J.-Y., Cowan, S.W., and Kjeldgaard, M. (1991). Improved methods for building protein models in electron density maps and the location of errors in these models. *Acta Crystallogr.* A47, 110–119.
- Lu, M., and Steitz, T.A. (2000). Structure of *E. coli* ribosomal protein L25 complexed with a 5S rRNA fragment at 1.8-Å resolution. *Proc. Natl. Acad. Sci. USA* 97, 2023–2028.
- Malkin, L.I., and Rich, A. (1967). Partial resistance of nascent polypeptide chains to proteolytic digestion due to ribosomal shielding. *J. Mol. Biol.* 26, 329–346.
- Mankin, A.S., and Garrett, R.A. (1991). Chloramphenicol resistance mutations in the single 23S rRNA gene of the archaeon *Halobacterium halobium*. *J. Bacteriol.* 173, 3559–3563.
- Milligan, R.A., and Unwin, P.N. (1986). Location of exit channel for nascent protein in 80S ribosome. *Nature* 319, 693–695.
- Moazed, D., and Noller, H.F. (1987). Interaction of antibiotics with functional sites in 16S ribosomal RNA. *Nature* 327, 389–394.
- Mueller, F., Sommer, I., Baranov, P., Matadeen, R., Stoldt, M., Woehnert, J., Grolach, M., van Heel, M., and Brimacombe, R. (2000). The 3D arrangement of the 23S and 5S rRNA in *E. coli* 50S ribosomal subunit based on a cryo-electron microscopic reconstruction at 7.5 Å resolution. *J. Mol. Biol.* 298, 35–59.
- Nakashima, T., Yao, M., Kawamura, S., Iwasaki, K., Kimura, M., and Tanaka, I. (2001). Ribosomal protein L5 has a highly twisted concave surface and flexible arms responsible for rRNA binding. *RNA* 7, 692–701.
- Navaza, J. (1994). AMoRe: an automated package for molecular replacement. *Acta Crystallogr.* A50, 57–163.
- Nikonov, S., Nevskaya, N., Eliseikina, I., Fomenkova, N., Nikulin, A.,

- Ossina, N., Garber, M., Jonsson, B.H., Briand, C., Al-Karadaghi, S., et al. (1996). Crystal structure of the RNA binding ribosomal protein L1 from *Thermus thermophilus*. *EMBO J.* *15*, 1350–1359.
- Nissen, P., Hansen, J., Ban, N., Moore, P.B., and Steitz, T.A. (2000). The structural basis of ribosome activity in peptide bond synthesis. *Science* *289*, 920–930.
- Noll, M., Hapke, B., Schreier, M.H., and Noll, H. (1973). Structural dynamics of bacterial ribosomes. I. Characterization of vacant couples and their relation to complexed ribosomes. *J. Mol. Biol.* *75*, 281–294.
- Ostergaard, P., Phan, H., Johansen, L.B., Egebjerg, J., Ostergaard, L., Porse, B.T., and Garrett, R.A. (1998). Assembly of proteins and 5 S rRNA to transcripts of the major structural domains of 23 S rRNA. *J. Mol. Biol.* *284*, 227–240.
- Otwinowski, Z., and Minor, W. (1997). Processing of X-ray diffraction data collected in oscillation mode. *Methods Enzymol.* *276*, 307–326.
- Penczek, P., Ban, N., Grassucci, R.A., Agrawal, R.K., and Frank, J. (1999). *Haloarcula marismortui* 50S subunit—complementarity of electron microscopy and X-ray crystallographic information. *J. Struct. Biol.* *128*, 44–50.
- Pioletti, M., Schlunzen, F., Harms, J., Zarivach, R., Gluhmann, M., Avila, H., Bashan, A., Bartels, H., Auerbach, T., Jacobi, C., et al. (2001). Crystal structures of complexes of the small ribosomal subunit with tetracycline, edeine and IF3. *EMBO J.* *20*, 1829–1839.
- Polacek, N., Gaynor, M., Yassin, A., and Mankin, A.S. (2001). Ribosomal peptidyl transferase can withstand mutations at the putative catalytic nucleotide. *Nature* *411*, 498–501.
- Porse, B.T., and Garrett, R.E.A. (1995). Mapping important nucleotides in the peptidyl transferase centre of 23S rRNA using a random mutagenesis approach. *J. Mol. Biol.* *249*, 1–10.
- Ryan, P.C., Lu, M., and Draper, D.E. (1991). Recognition of the highly conserved GTPase center of 23 S ribosomal RNA by ribosomal protein L11 and the antibiotic thiostrepton. *J. Mol. Biol.* *221*, 1257–1268.
- Sabatini, D.D., and Blobel, G. (1970). Controlled proteolysis of nascent polypeptides in rat liver cell fractions. Location of the polypeptides in rough microsomes. *J. Cell Biol.* *45*, 146–157.
- Schlunzen, F., Tocilj, A., Zarivach, R., Harms, J., Gluehmann, M., Janelli, D., Bashan, A., Bartels, H., Agmon, I., Franceschi, F., and Yonath, A. (2000). Structure of functionally activated small ribosomal subunit at 3.3 angstroms resolution. *Cell* *102*, 615–623.
- Schlunzen, F., Zarivach, R., Harms, J., Bashan, A., Tocilj, A., Albrecht, A., Yonath, A., and Franceschi, F. (2001). Structural basis for the interaction of chloramphenicol, clindamycin, and macrolides with the peptidyl transferase center in eubacteria. *Nature* *413*, 814–821.
- Sonenberg, N., Wilchek, M., and Zamir, A. (1973). Mapping of *E. coli* ribosomal components involved in peptidyl transferase activity. *Proc. Natl. Acad. Sci. USA* *70*, 1423–1426.
- Subramanian, A.R., and Dabbs, E.R. (1980). Functional studies on ribosomes lacking protein L1 from mutant *E. coli*. *Eur. J. Biochem.* *112*, 425–430.
- Thompson, J., Kim, D.F., O'Connor, M., Lieberman, K.R., Bayfield, M.A., Gregory, S.T., Green, R., Noller, H.F., and Dahlberg, A.E. (2001). Analysis of mutations at residues A2451 and G2447 of 23S rRNA in the peptidyltransferase active site of the 50S ribosomal subunit. *Proc. Natl. Acad. Sci. USA* *98*, 9002–9007.
- Unge, J., Berg, A., Al-Kharadaghi, S., Nikulin, A., Nikonov, S., Davydova, N., Nevskaya, N., Garber, M., and Liljas, A. (1998). The crystal structure of ribosomal protein L22 from *Thermus thermophilus*: insights into the mechanism of erythromycin resistance. *Structure* *6*, 1577–1586.
- Wahl, M.C., Bourenkov, G.P., Bartunik, H.D., and Huber, R. (2000). Flexibility, conformational diversity and two dimerization modes in complexes of ribosomal protein L12. *EMBO J.* *19*, 174–186.
- Walleczek, J., Martin, T., Redl, B., Stoffer-Meilicke, M., and Stoffer, G. (1989). Comparative cross-linking study on the 50S ribosomal subunit from *E. coli*. *Biochemistry* *28*, 4099–4105.
- White, O., Eisen, J.A., Heidelberg, J.F., Hickey, E.K., Peterson, J.D., Dodson, R.J., Haft, D.H., Gwinn, M.L., Nelson, W.C., Richardson, D.L., et al. (1999). Genome sequence of the radioresistant bacterium *Deinococcus radiodurans* R1. *Science* *286*, 1571–1577.
- Wimberly, B.T., Guymon, R., McCutcheon, J.P., White, S.W., and Ramakrishnan, V. (1999). A detailed view of a ribosomal active site: the structure of the L11-RNA complex. *Cell* *97*, 491–502.
- Wimberly, B.T., Brodersen, D.E., Clemons, W.M., Jr., Morgan-Warren, R.J., Carter, A.P., Vornrhein, C., Hartsch, T., and Ramakrishnan, V. (2000). Structure of the 30S ribosomal subunit. *Nature* *407*, 327–339.
- Wittmann, H.G. (1983). Architecture of prokaryotic ribosomes. *Annu. Rev. Biochem.* *52*, 35–65.
- Worbs, M., Huber, R., and Wahl, M.C. (2000). Crystal structure of ribosomal protein L4 shows RNA-binding sites for ribosome incorporation and feedback control of the S10 operon. *EMBO J.* *19*, 807–818.
- Wower, I.K., Wower, J., and Zimmermann, R.A. (1998). Ribosomal Protein L27 Participates in both 50 S Subunit Assembly and the Peptidyl Transferase Reaction. *J. Biol. Chem.* *273*, 19847–19852.
- Yonath, A., Leonard, K.R., and Wittmann, H.G. (1987). A tunnel in the large ribosomal subunit revealed by three-dimensional image reconstruction. *Science* *236*, 813–816.
- Yusupov, M.M., Yusupova, G.Z., Baucom, A., Lieberman, K., Earnest, T.N., Cate, J.H., and Noller, H.F. (2001). Crystal structure of the ribosome at 5.5 Å resolution. *Science* *292*, 883–896.

#### Accession Numbers

The coordinates have been deposited at the Protein Data Bank under PDB accession code 1KC9.

Note: While this manuscript was reviewed, the refined coordinate set of H50S was submitted to the Protein Data Bank (accession code 1JJ2). The new entry contains coordinates for helices 43/44 that were considered disordered in Ban et al., 2000. We relate to these features in Table S1 and in the discussions about the L7/L12 stalk and the peptidyl transferase activity.